

# The Stability of Insulin in Crystalline and Amorphous Solids: Observation of Greater Stability for the Amorphous Form

Michael J. Pikal<sup>1,2,3</sup> and Daniel R. Rigsbee<sup>1</sup>

Received March 17, 1997; accepted June 20, 1997

**Purpose.** Generalizations based upon behavior of small molecules have established that a crystalline solid is generally much more stable toward chemical degradation than is the amorphous solid. This study examines the validity of this generalization for proteins using biosynthetic human insulin as the model protein.

**Methods.** Amorphous insulin was prepared by freeze drying the supernate from a suspension of zinc insulin crystals adjusted to pH 7.1. Storage stability at 25°C and 40°C were compared for the freeze dried material, the dried suspended crystals, and the starting batch of crystals. Samples were equilibrated at selected relative humidities between zero and 75% to obtain samples at various water contents. Assays for dimer formation were performed by size exclusion HPLC and assays for deamidated product were carried out by reverse phase HPLC. Degradation was found to be linear in square root of time, and the slopes from % degradation vs. square root of time were used to define the rate constants for degradation. Differential scanning calorimetry (DSC) and Fourier-transform infrared spectroscopy (FTIR) were used to characterize the state of the protein in the solids.

**Results.** As expected based upon previous results, the primary degradation pathways involve deamidation at the Asn<sup>A21</sup> site and co-valent dimer formation, presumably involving the A-21 site. Contrary to expectations, amorphous insulin is far more stable than crystalline insulin under all conditions investigated. While increasing water content increases the rate of degradation of crystalline insulin, rate constants for degradation in the amorphous solid are essentially independent of water content up to the maximum water content studied ( $\approx 15\%$ ).

**Conclusions.** Based upon the FTIR and DSC data, both crystalline and amorphous insulin retain some higher order structure when dried, but the secondary structure is significantly perturbed from that characteristic of the native solution state. However, neither DSC nor FTIR data provide a clear interpretation of the difference in stability between the amorphous and crystalline solids. The mechanism responsible for the superior stability of amorphous insulin remains obscure.

**KEY WORDS:** insulin; protein stability; solid-state degradation; deamidation; dimerization; water effects; differential scanning calorimetry; Fourier-transform infrared spectroscopy; protein conformation in solids.

## INTRODUCTION

It has long been recognized that a crystalline drug is normally much more stable toward chemical degradation than the

corresponding amorphous solid. Differences of more than an order of magnitude are common for small molecules (i.e., non-proteins). (1–3). This observation is likely a result of the crystalline environment providing an inert and “rigid” environment for the molecule that does not readily allow the motion needed for reactions to occur. The few known examples of greater reactivity in the crystalline state arise from situations where the crystal structure forces the close proximity of two reactive centers, such that reaction may occur with minimal motion (4).

The greatly enhanced stability of the crystalline state observed for small molecules may not translate to proteins. While inter-molecular interactions in the crystal lattice that reduce mobility involve a significant fraction of the functional groups with a typical small molecule, most of the inter-residue interactions in a protein are intra-molecular. Thus, the additional order, reduction in free volume, and reduced mobility in the crystalline state should be much less pronounced for a protein than with a small molecule, and the resulting stability advantage of the crystalline form should be less. The observation that aqueous suspensions of crystalline insulin are only slightly more stable (i.e., about a factor of two) than the corresponding suspensions of amorphous phase (5) supports the above speculation. A crystalline protein should also be more stable because the solid state conformation should be “more native”. Protein structure studies by x-ray diffraction assume that, at least for a fully hydrated protein, the solid state conformation is native. However, the conformation of a freeze dried amorphous protein is often significantly perturbed, and stability of the freeze dried protein correlates with how closely the solid state conformation resembles the “native” solution conformation (6,7).

Although the preceding discussion suggests that the stability of a crystalline protein will be greater than the stability of the amorphous form, supporting data is meager. This research is a detailed investigation of the stability differences between a crystalline protein, insulin, and the corresponding freeze dried amorphous form as a function of water content and temperature. Insulin was chosen as the model protein largely because highly purified crystalline material is readily available, highly precise HPLC assays are available to evaluate degradation, and the major degradation pathways have been relatively well characterized (5,8,9–11). To supplement stability studies, the physical state of insulin in the solid state was investigated using both differential scanning calorimetry (DSC) and Fourier-Transform-Infrared Spectroscopy (FTIR). Surprisingly, we find that, at all conditions studied, freeze dried amorphous insulin is considerably more stable than crystalline insulin.

## MATERIALS AND METHODS

### Materials

Biosynthetic human insulin was obtained as crystalline “2-zinc” bulk drug (Eli Lilly & Co), which is prepared by crystallization near the isoelectric point from a zinc containing solution. Additional samples were prepared to provide crystals and freeze dried material at the same effective pH.<sup>4</sup> The bulk

<sup>4</sup> Addition of 3 ml water to 14 mg of each solid, and separation of the remaining crystals, gave pH values for the respective solutions of: 7.3 (freeze dried), 7.1 (“pH7 crystals”), and 6.6 (“QA crystals”).

<sup>1</sup> Lilly Research Laboratories, Eli Lilly & Co., Indianapolis, Indiana 46285.

<sup>2</sup> Current Address: University of Connecticut, School of Pharmacy, 372 Fairfield Road, U-92, Storrs, Connecticut 06269-2092. (e-mail: pikal@uconnvm.uconn.edu)

<sup>3</sup> To whom correspondence should be addressed.

crystalline drug was suspended in water, the pH adjusted to and maintained at pH 7.1 by titration with 0.1N NaOH while stirring slowly for 3.5 hours. The solution (4.7 mg/ml insulin) was separated from the remaining crystals by filtration, filled into 5 cc glass vials (3 ml fill volume), and freeze dried as described below. The remaining crystals were dried in a vacuum oven at 25°C for 8 hours, followed by 35°C vacuum drying for 1 hour. These "pH7 crystals" and the starting bulk crystalline material, denoted "QA crystals", were filled into 5 cc glass vials ( $\approx 30$  mg/vial). The crystalline samples and the freeze dried samples were then stored for several days in vacuum desiccators containing saturated salt solutions to provide the appropriate relative humidity for moisture equilibration or containing drierite to provide zero relative humidity.

### Freeze Drying Procedures

Freeze drying was performed with a Virtis 25 SRC-X freeze dryer. Freezing was initiated by cooling the vial contents on the freeze dryer shelves to about  $-10^\circ\text{C}$ , where ice nucleated and freezing began uniformly throughout the vial. After ice formation began, the product was cooled to  $-45^\circ\text{C}$  within about 30 minutes to complete the freezing process. The product temperature was maintained at  $\approx -35^\circ\text{C}$  throughout primary drying ( $\approx 24$  hours). The final stage of secondary drying was carried out at a product temperature of 25°C for 5 hours. The samples freeze dried without any evidence of collapse.

### Physical Measurements

Differential scanning calorimetry (DSC) studies were carried out using a Perkin-Elmer DSC-7 at a scan rate of  $10^\circ\text{C}/\text{min}$ . The powder samples (5–8 mg) were compacted into thin (1–2 mm) disks of about 3 mm diameter to increase the amount of sample one could place into the sealed aluminum DSC pans as well as to increase heat transfer from the pan to the sample. All sample handling was carried out in a "dry bag" continuously purged with air at the relative humidity corresponding to the equilibration relative humidity of the samples.

The FTIR spectra were collected on a Nicolet model 550 Magna series spectrometer using procedures similar to those described by other workers (12,13). For the solid samples, 1 to 2 mg of the protein was lightly ground with 350 mg of KBr powder and made into a pellet. The reported data represent smoothed second derivative spectra. The area under the curve

within the amide I region (1600 to  $1700\text{ cm}^{-1}$ ) was determined after baseline correction and was normalized for the purpose of lot to lot comparisons.

For the FTIR solution state denaturation experiment, an 18 mg/ml solution of lyophilized insulin in 10 mM potassium phosphate buffer (pH 7.4) was centrifuged, and the supernatant was loaded into a cell using a 6 micron spacer. Spectra were obtained from 25°C to 85°C in 10 degree increments, with data collected for 20–25 min. after thermal equilibrium. After correcting for the blank (i.e., buffer alone), data were analyzed as described above.

The water sorption isotherms were determined gravimetrically using a microbalance procedure. Briefly, a sample ( $\approx 10$  mg) was loaded into a quartz pan, and the sample was exposed to high vacuum ( $\approx 10^{-6}$  Torr) at 25°C until the rate of mass loss slowed to  $\approx 2\ \mu\text{g}/\text{hr}$  to obtain the anhydrous sample mass. The sample, maintained at 25°C, was then exposed to water vapor from a temperature controlled sample of water (or ice) to allow equilibration. Equilibration was assumed when the rate of mass gain was less than  $\approx 2\ \mu\text{g}/\text{hr}$ . After equilibration, the temperature of the water source was increased, and the equilibration process was repeated until the desired sorption isotherm was obtained.

### Assays: Characterization of Degradation Rates

#### HPLC Assay Methodology

Insulin related substances were determined by reversed phase gradient HPLC using two methods (14). Method 1 measures deamidation at the A21 site as well as aggregation but does not separate deamidation at the B3 site from the insulin main peak. Here, the column was a Vydac Protein and Peptide  $C_{18}$  thermostated to 40°C. The mobile phases A (82% buffer) & B (50% buffer) consist of mixtures of sodium sulfate buffer (pH to 2.3 with phosphoric acid) and acetonitrile. The gradient program began isocratic at 22% B for 35 minutes with solvent B increased at 1.8% per minute for 25 minutes and held constant for 6 minutes before reequilibrating to initial conditions. The detector was set to 214 nm. Solutions were prepared by dissolving an accurately weighed 3 mg portion of the solids with 1 ml 0.01N HCl. The samples were placed on a refrigerated autosampler. A 20  $\mu\text{l}$  injection volume was used. The related substances peak areas were compared against a calibration curve of dilute insulin standards.

Another reversed phase gradient method (14), denoted "method 2", was used to determine the amount of "B3 deasamido". A 0.2M ammonium phosphate buffer was prepared and adjusted to pH 7.0. Solvent A was 50:40:10 buffer:water:acetonitrile. Solvent B was 50:50 buffer:acetonitrile. The program began at 37%B and remained isocratic for 15 minutes. Solvent B was then stepped to 40%, then to 43%; each step isocratic for 15 min. Next, the composition of B was increased by 1.3% per min for 20 min at which time it was held isocratic for 5 min before returning to initial values. The column used was the Beckman Ultrasphere ODS, 5 micron. Operating conditions, sample preparation, sample handling, and analysis were the same as those in the first method.

The percentage of soluble protein aggregates was determined by an isocratic size exclusion HPLC method (14). The column was a Dupont Zorbax GF250 at ambient temperature

---

Microscopic examination showed that both crystalline preparations were birefringent, and therefore, apparently at least mostly crystalline. The freeze dried sample was non-birefringent and "glassy" with morphology typical of freeze dried amorphous materials. While the "pH7 crystals" did appear crystalline, the crystals were somewhat deformed, suggesting that the preparation introduced some amorphous phase. Solubility measurements gave the following solubilities at room temperature: freeze dried,  $>5.2\ \text{mg}/\text{ml}$ ; "pH7 crystals",  $0.2\ \text{mg}/\text{ml}$ ; "QA crystals",  $0.05\ \text{mg}/\text{ml}$ . The higher solubility of the "pH7 crystals" relative to the "QA crystals" could arise from the higher state of ionization (i.e., the higher effective pH) and/or contamination by amorphous phase. Assuming the higher solubility arises solely from amorphous phase contamination yields an estimate for the upper limit of amorphous phase content of about 4%. Thus, it seems clear that the "pH7 crystals" are mostly crystalline with at most a trace of amorphous phase contamination.

with a mobile phase of 0.4M ammonium bicarbonate at flow rate 0.5 ml/min. Samples at a relatively high concentration (3 to 3.5 mg/ml) were diluted to 1% with 0.01N HCl. These were used as standards for the high concentration samples. Results were expressed as a percentage of the standard main peak.

#### Water Content Assay

Moisture contents were determined by coulometric Karl Fischer methods. Exposure of a crystalline sample to the environment was minimized by weighing the sample and container, quickly dumping sample into the titrator, and re-weighing. For lyophilized samples, low density required a method using anhydrous methanol as a "carrier". The sample was dissolved methanol of known low moisture and an aliquot of solution was injected into the titrator. Empty vials, equilibrated to the same relative humidities as the corresponding sample, were run for the blank determination.

#### Characterization of Degradation Rates

Samples were stored at 40°C (0.5, 1, 2 months) and at 25°C (1, 3, 6 months). Assays for co-valent dimer via size exclusion HPLC and assay for A21 deamidation (method 1) were run at each time point, while assays for B3 deamidation (method 2) were run only on the initial and final time points for each temperature. Two independent replicate samples were assayed for each time/temperature data point.<sup>5</sup>

Total degradation measured by reverse phase HPLC, degradation via A21 deamidation, and dimer formation (SEC HPLC) were found to be consistent with "square root of time" kinetics. That is, the percent degradation product(s), %P, follows the linear equation,

$$\%P = P_0 + k \sqrt{t} \quad (1)$$

where  $P_0$  is initial level of degradation product(s) and "k" is the effective rate constant. In general, the data fit equation 1 nearly within the precision of the assay, with the square of the correlation coefficient averaging about 0.98. However, small systematic deviations from eq 1 were apparent, particularly with dimer formation at 40°C in samples equilibrated with 75% relative humidity. A better fit would have been obtained with a quadratic fit in  $\sqrt{t}$  with a positive coefficient for the term in "t". However, to remain consistent in the data analysis, and to limit the number of fitted parameters, all data were fit to eq 1 to derive experimental values of apparent rate constants, k. While eq 1 is an empirical result, as will be discussed later, at least two theoretical models do predict "square root of time kinetics" under the conditions of these experiments.

<sup>5</sup> The mean difference between replicate samples was 0.03% for B3-desamido assays, and for A21 desamido and dimer assays, the mean difference ranged from about 0.02% for "initial" samples to about 0.09% for the final time points at each temperature. During each sequence of assays, a "referee" lot, stored at -20°C, was assayed to detect potential long term drift in the assay. No long term drift was detected; the standard deviation of the assays on the referee lot was about  $\pm 0.01\%$  for the B3 desamido assay and about  $\pm 0.05\%$  for the A21 desamido and dimer assays.

## RESULTS AND DISCUSSION

### Water Sorption Isotherms

Water sorption isotherms measured at 25°C are shown in Figure 1 for both the freeze dried amorphous insulin and the "QA" crystals. The qualitative features of the two sorption isotherms are essentially the same, with the amorphous form absorbing slightly more water at a given relative humidity. A BET (Brunauer-Emmitt-Teller) analysis of the data between 5% and 30% relative humidities gives "monolayer" coverages of 5.4% (freeze dried) and 4.3% ("QA" crystals), both "monolayer" coverages corresponding to relative humidities of about 24%. Strickley and Anderson (11) find  $\approx 4.6\%$  water for BET "monolayer" coverage for insulin freeze dried from acidic solutions. The difference between their result and our result for amorphous insulin (i.e., 5.4% vs. 4.6%) is likely a reflection of the difference in sample pH.

The "monolayer" level of water is of potential significance for stability in that one can argue (15) that at a moisture content near "monolayer", reactive groups in the protein as well as potential reactants, such as water, acquire sufficient mobility to facilitate degradation processes. Thus, one might expect a sharp increase in degradation rate near the "monolayer" level of water.

### Differential Scanning Calorimetry

Several examples of differential scanning calorimetry (DSC) data are illustrated by Figure 2. The thermograms are characterized by denaturation endotherms, marked with "\*", and very broad and weak endotherms of uncertain origin marked with a question mark, "?". On the time scale of the DSC experiment, both types of endotherm are irreversible. That is, if a sample is scanned through the endotherm and then cooled and re-scanned, the second scan does not show the endotherm. The broad endotherms become stronger and shift to slightly lower temperature with increasing hydration. Similar broad endotherms were observed during DSC studies of freeze dried human growth hormone (16,17). We suggest that these broad endotherms represent enthalpy relaxation in the solid. It is well

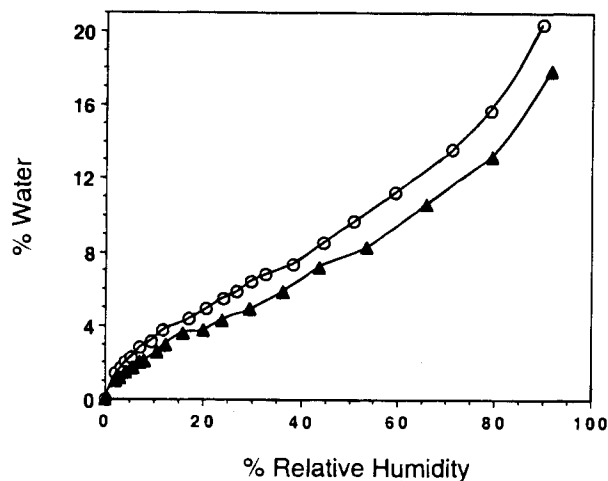


Fig. 1. Water Sorption Isotherms of Freeze Dried and Crystalline Insulin at 25°C. Key: open circles = freeze dried amorphous; filled triangles = crystalline (QA crystals).

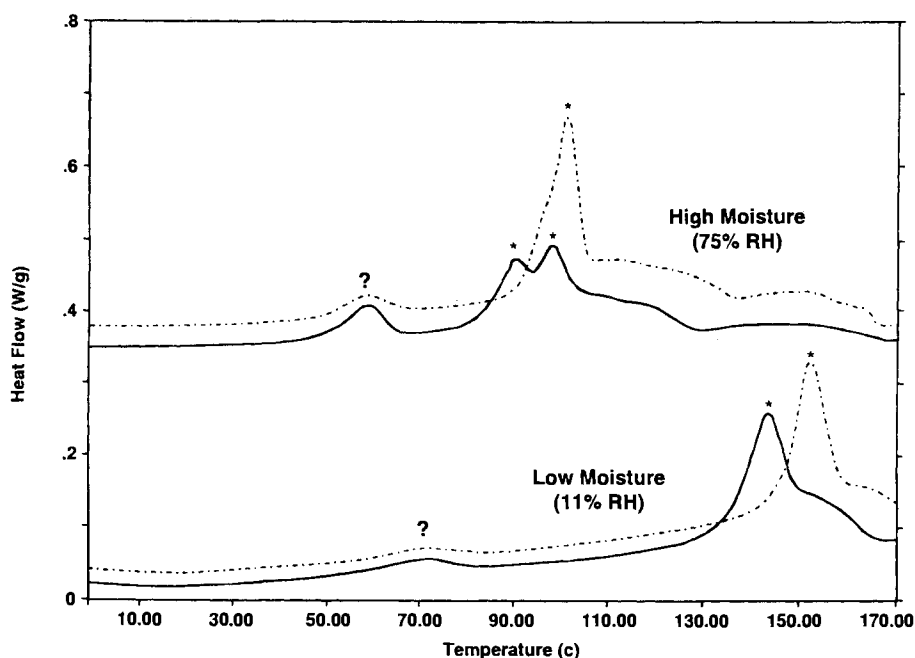


Fig. 2. Differential Scanning Calorimetry of Amorphous and Crystalline Insulin Samples Equilibrated at 11% Relative Humidity and 75% Relative Humidity. The crystalline samples are "pH 7" crystals. The notation, "\*", indicates denaturation endotherms while the question marks, "?", denote the broad endotherms suspected to arise from enthalpy relaxation.

known (18–20) that glassy solids undergo structural changes when aged, where the metastable structure "frozen in" during preparation relaxes toward a lower energy state characteristic of the storage temperature. When a DSC scan is performed on such a relaxed sample, the energy lost during aging is regained as soon as mobility in the solid is sufficiently rapid to allow the change in structure on the time scale of the DSC scan, which is typically at the glass transition temperature but may also be below the glass transition (19). Thus, the DSC scan shows a relaxation enthalpy endotherm superimposed on the heat capacity increase at the glass transition or alternately, an "enthalpy relaxation" endotherm appears below the glass transition. However, with insulin, as well as with pure human growth hormone (16,17), bovine somatotropin (21) and several other proteins (19,22), the sharp increase in baseline characteristic of the glass transition is absent from the DSC data. Specifically, for insulin (Figure 2), there is *not* a change in baseline near or above the broad endotherm that could be attributed to the change in heat capacity at the glass transition. While a glass transition could be hidden in the onset of the denaturation endotherm, it is more likely that, like other proteins (19,23), insulin is a "strong glass" with a very small heat capacity change corresponding to the glass transition. A strong glass means, effectively, that the glass transition occurs over a very broad range of temperature. Thus, the glass transition in insulin is broad and weak and cannot be detected by conventional DSC. Since unfolding on the time scale of the DSC experiment is very unlikely below the glass transition temperature (3), the glass transition temperature of insulin likely lies somewhere between the denaturation temperature and the temperature of the broad endotherm we interpret as the relaxation enthalpy endotherm. Provided our interpretation of the broad endotherms is substantially correct, it is clear that, solid insulin samples

are below their glass transition temperatures at room temperature, and insulin in the glassy state does have structural mobility on the time scale the samples were stored (i.e., days-weeks). Furthermore, although enthalpy relaxation is classically associated with amorphous solids, it appears that crystalline proteins also undergo a similar process.

The irreversible character of the denaturation endotherm is a common feature of protein denaturation in the solid state (21–23) and likely is a result, at least in part, of the extensive degradation that occurs (21) when a protein unfolds at high temperature. While denaturation could be either kinetically or thermodynamically controlled,<sup>6</sup> it is clear that denaturation does occur, which means that the dried protein does have higher order structure. Thus, insulin is not completely unfolded during drying. While, in general, the denaturation endotherms appeared to be single roughly symmetrical peaks, samples at high moisture content (i.e., 75% relative humidity) appear to denature in a two step process. That is, particularly for amorphous insulin at 75% relative humidity, the denaturation endotherm is really two endotherms. However, the possibility of kinetic control of denaturation obscures the meaning of this observation.

Figure 3 gives the variation of the apparent heat of denaturation and denaturation temperature with water content. Crystalline insulin has a higher heat of denaturation than amorphous

<sup>6</sup> In this context, thermodynamic control means that the denaturation temperature is, at least approximately, the temperature at which the free energy of unfolding is zero. Complete kinetic control prevails when the free energy of unfolding passes through zero at a much lower temperature than the denaturation temperature, but denaturation occurs only when the rate of unfolding becomes comparable to the scan rate (24).

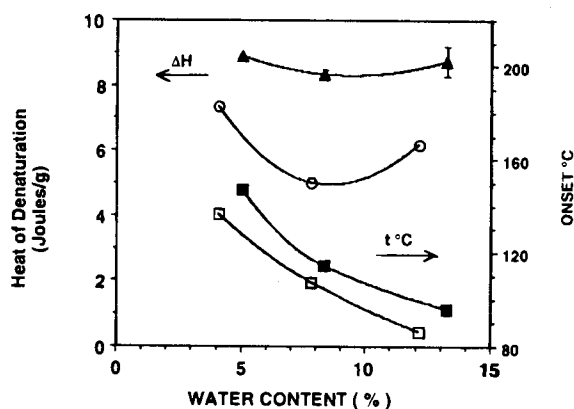


**Fig. 3.** Variation of the Denaturation Temperature and Effective Heat of Denaturation with Water Content for Amorphous and Crystalline Insulin. Key: triangles and circles = heats of denaturation in J/g; squares = temperature of denaturation onset; open symbols = freeze dried amorphous; filled symbols = crystalline (pH 7 crystals).

insulin at all water contents. This observation is consistent with greater retention of conformational structure by the crystalline insulin during drying. One could also argue that this result is a consequence of differing contributions to the apparent heat of denaturation arising from exothermic degradation during unfolding. However, since the denaturation temperatures are systematically higher for crystalline insulin, and amorphous insulin is significantly more stable than crystalline insulin at lower temperatures (as will be discussed later), it is more likely that degradation would be more severe for crystalline insulin, thereby causing the heat of denaturation of the crystalline phase to be smaller than for the amorphous phase, which is opposite from the observed difference. It should also be noted that, for both crystalline and amorphous phases, increasing water content lowers the denaturation temperature in roughly the same manner. The effect of water content on denaturation temperature is similar to that observed for other proteins (21,23).

### Infrared Spectroscopy

Second derivative, area normalized, FTIR spectra in the Amide I region are compared in Figure 4 for aqueous, dry crystalline, and dry amorphous insulin. It is obvious that while the spectra for the two solids are similar, the spectrum for the solution is quite different. Deconvolution into gaussian components (deconvolution data not shown) gives six major bands for each spectrum.<sup>7</sup> All solid bands are broader than the corresponding solution bands, particularly for the alpha helix band (1659  $\text{cm}^{-1}$ ) and the 1689  $\text{cm}^{-1}$  beta sheet band where the

<sup>7</sup> For the solution spectrum, the band positions ( $\text{cm}^{-1}$ ) and their tentative assignments (12) are: 1614 (side chain), 1637 (beta sheet), 1649 (random coil), 1659 (alpha helix), 1678 (beta turn), and 1689 (beta sheet). For the solids, band positions and assignments are: 1614 (side chain and beta sheet), 1632 (beta sheet), 1642 (beta sheet), 1658 (alpha helix), 1683 (beta turn), and 1659 (beta sheet). Since drying appears to shift beta sheet bands to slightly higher wave numbers (25), the 1642  $\text{cm}^{-1}$  band in the dried solids likely corresponds to the 1637 band in the solution spectrum rather than the 1649  $\text{cm}^{-1}$  band in the solution spectrum.

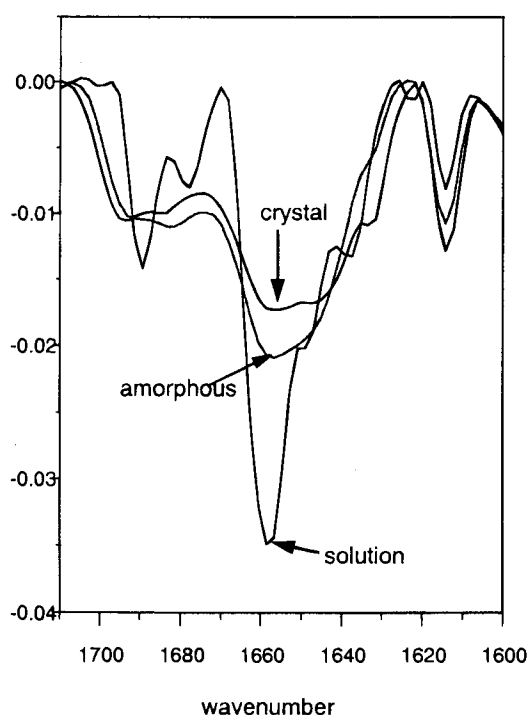


**Fig. 4.** FTIR Spectra of Aqueous, Crystalline, and Amorphous Insulin in the Amide I Region. Spectra are second derivative, area normalized spectra taken at room temperature. The solids were nominally dry. The solution was 18 mg/ml insulin, buffered with 10 mM potassium phosphate at pH 7.4.

widths in the solid spectra are more than twice those observed in the solution. The major differences between the solution spectrum and the solid spectra are that the helix band is reduced in intensity and broadened in the solid spectra relative to the solution spectrum, and the random coil band (1649  $\text{cm}^{-1}$ ) is not observed in the solid spectra. For the solution spectrum, deconvolution gives the contribution of each type of secondary structure as (% of total with side chain area subtracted): helix (40%), beta sheet/turn (32%), random coil (28%). An analysis of circular dichroism data at pH 7 (26) gives a helix content of 42%, which is very close to our FTIR spectroscopic value. The alpha helix band areas are nearly identical for solution (40%), and crystalline solid (41%), and slightly higher for the freeze dried solid (50%). The total areas of the beta sheet/turn bands are: 32% (solution), 59% (crystalline), and 50% (freeze dried). Thus, the major qualitative effect of drying on secondary structure is to create beta sheet/turn at the expense of random coil. With the freeze dried form, a small amount of alpha helix is also created. In this sense, drying *increases* structure, an observation also made recently by other workers (27). However, it must be emphasized that the sizable broadening of the helix band with corresponding decrease in intensity is a loss of structure in the sense that the number of distinct helix states is increased.

The temperature dependence of the solution spectra were studied between 25°C and 85°C (data not shown). The major changes occur between 75°C and 85°C where the alpha helix band sharply decreases in intensity and broadens. In addition, a strong beta sheet band appears at about 1625  $\text{cm}^{-1}$ , other beta sheet bands intensify, and the beta sheet band at 1689

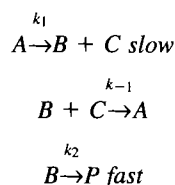
$\text{cm}^{-1}$  decreases in intensity. The net result is that the spectrum of the denatured insulin (i.e., 85°C spectrum) resembles the spectra of the solids (Figure 4). Thus, from this viewpoint, the dried solids are significantly denatured. It should be noted that the FTIR data do not support the speculation, based upon heats of denaturation (Fig. 3), that the crystalline form is "more native" than the amorphous form. However, since FTIR data reflect changes in secondary structure only, and heats of denaturation reflect changes in both secondary and tertiary structure, the FTIR data do not contradict the suggestion that the crystalline form is slightly "more native".

## Chemical Stability

### Square Root of Time Kinetics

The rate of formation of degradation products decreases with increasing time, and as a first approximation, degradation appears to be linear in square root of time (eq 1). We now describe two "mechanisms" which can lead to such behavior.

If it is assumed that the degradation of a compound, "A", proceeds through an intermediate, denoted "B", to form product "P" according to the general scheme,



the resulting set of differential equations may be solved with the boundary condition,  $C_A(t=0) = 1$ , ( $C_A$  = "concentration of species "A") to give

$$t = -\left(\frac{1}{k_1} + \frac{k_{-1}}{k_1 k_2}\right) \cdot \ln C_A - \left(\frac{k_{-1}}{k_1 k_2}\right) \cdot (1 - C_A) \quad (2)$$

If we further assume,  $k_{-1} \gg k_2$ , and restrict application to situations of slight degradation,  $C_p = (1 - C_A) \ll 1$ , eq 2 reduces to the form,

$$C_p = \sqrt{\frac{2k_1 k_2}{k_{-1}}} \cdot \sqrt{t} \quad (3)$$

In the case of several reaction products, as with insulin, the concentration of reaction product "P",  $C_{pi}$ , is given by a generalization of eq 3,

$$C_{pi} = k_{2i} \sqrt{\frac{2k_1}{k_2 k_{-1}}} \cdot \sqrt{t}; \quad k_2 = \sum_i k_{2i} \quad (4)$$

Equation 4 is equivalent to eq 1, where the experimental rate constant defined by eq 1 is really a combination of rate constants. At least for insulin, the equilibrium model defined by scheme II is quite reasonable since it has been shown that degradation of insulin in the solid state does proceed via a cyclic anhydride intermediate (11). Thus, in scheme II, species "B" is the cyclic intermediate, species "C" is ammonia, and species "P" represents one of the several reaction products possible.

An alternate model could also lead to "square root of time kinetics". If the protein exists in a number of configurations,

each configuration degrading in first order fashion with a different rate constant, the equation describing the concentration of starting material as a function of time would be a multi-exponential decay function of the form,

$$C_A = \sum_i C_{Ai}^0 \cdot \exp(-k_i t) \quad (5)$$

where  $C_{Ai}^0$  is the initial concentration of "A" in configuration "i", and  $k_i$  is the rate constant for degradation of the "i<sup>th</sup>" configuration. From a mathematical viewpoint, this model is similar to "multi-state" structural relaxation in glassy solids, where relaxation to a lower energy state proceeds via a multi-exponential decay with the same form as eq 5 but with concentration replaced by energy. Empirically, such a multi-exponential decay may be described by the "stretched exponential" or "Kohlraush-Williams-Watts equation (20,28)

$$1 - \frac{\Delta H_r(t)}{\Delta H_r(t=\infty)} \equiv \Phi(t) = \exp\left[-\left(\frac{t}{\tau}\right)^\beta\right] \quad (6)$$

where  $\Delta H_r(t)$  is the enthalpy of relaxation at time  $t$ ,  $\tau$  is a "mean" relaxation time (i.e., a reciprocal of a rate constant), and  $\beta$  is the "stretched exponential" constant which is between zero and unity. For a single relaxation mode,  $\beta = 1$ , but for a wide distribution of relaxation times (i.e., wide distribution of rate constants),  $\beta$  decreases from unity, and often is on the order of 0.5. Application of eq 6 to protein degradation (i.e., eq 5), proceeds by identification of,  $C_A = \Phi(t)$ , rate constant,  $k_s = 1/\tau$ , and if degradation is slight, expansion of the exponential in eq 6 then gives,

$$C_p = (k_s)^\beta (t)^\beta \quad (7)$$

where if  $\beta \approx 0.5$ , eq 7 gives "square root of time kinetics", with the rate constant defined by eq 1 being a fractional power of an "average" rate constant for the various populated configurations.

### Stability Comparisons: Crystalline vs. Amorphous as a Function of Water Content

Size exclusion HPLC chromatograms are relatively simple; more than 90% of all covalent aggregates are dimers. Reverse phase chromatograms contain desamido peaks, and as found in previous studies (9,11,29) a collection of sharp peaks believed to represent dimer species appears at high retention times. Previous studies (9,11) suggest that Asn<sup>A21</sup>-Phe<sup>B1</sup> and Asn<sup>A21</sup>-Gly<sup>A1</sup> dimers are the major products. The distribution of insulin degradation products after 2 months storage at 40°C is shown in Figure 5. The classification, "other", refers to degradation measured by reverse phase "method 1" which is not A-21 desamido minus the dimer level as determined by size exclusion HPLC. In general, dimers are the dominant degradation product, and Asn<sup>A21</sup> is the dominant deamidation site. Only with amorphous insulin at high relative humidity is deamidation at the B-3 site more prevalent than A-21 deamidation. Both crystalline forms show greater degradation at 75% relative humidity than when dry, but except for deamidation at the B-3 site, degradation of amorphous insulin shows little sensitivity to moisture content. Most surprising, A-21 deamidation, dimer formation, as well as total degradation (not shown) are more extensive in both crystalline forms than in the freeze dried amorphous form.

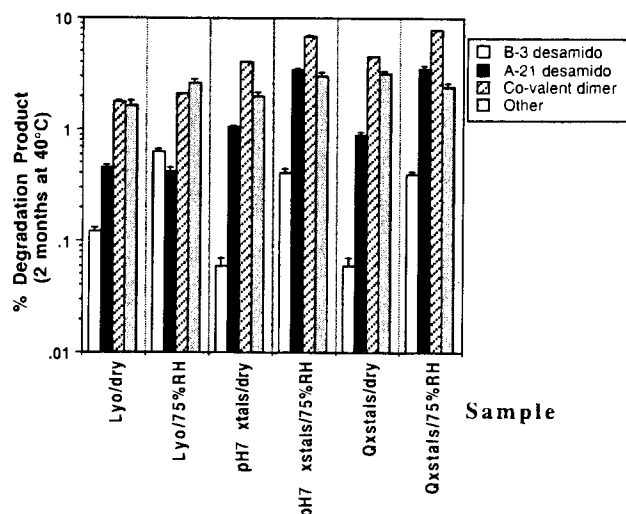


**Fig. 5.** Distribution of Insulin Degradation Products after 2 months Storage at 40°C. "Lyo" = freeze dried amorphous; "pH7 xtals" = pH 7 crystalline solids; "Qxtals" = "QA" crystalline solids. Co-valent dimer data are from size exclusion HPLC assays, A-21 desamido is A-21 deamidated product determined from the "Method 1" reversed phase HPLC assay, B-3 desamido is B-3 deamidated product from the "Method 2" reversed phase HPLC assay. The data denoted, "other", is the difference between the total degradation measured by the "Method 1" reversed phase assay and the sum of the A-21 desamido product and the size exclusion dimer content. Initial levels of degradation products in the freeze dried solids were: 0.46% A-21 desamido, 0.34% dimer (SEC), 0.3% other. Corresponding initial levels for the crystalline solids were: 0.63%, 0.51%, and 0.4%.

The relationship between degradation rate, water content, and solid form is explored in more detail by Figure 6 (A-21 deamidation) and Figure 7 (dimer formation by SEC HPLC). The rate constants according to eq 1 (i.e., square root of time kinetics) are shown for both 40°C storage and 25°C storage.<sup>8</sup> It is obvious that for all water contents studied, freeze dried amorphous insulin is considerably more stable than either crystalline form at both 25°C and 40°C. For crystalline forms, deamidation at the A-21 site increases sharply as the moisture content increases. This result is expected since water is a reactant in the deamidation process (11), and one might expect greater configurational flexibility at higher moisture contents (15). However, for amorphous insulin, deamidation at the A-21 site is nearly independent of moisture, the only effect being a slight decrease in rate constant at higher moisture levels. Likewise, the rate of dimer formation in amorphous insulin is nearly independent of water content. Total degradation in amorphous insulin is essentially independent of water content over the range studied. For crystalline insulin, the effect of water content on dimer formation is somewhat more complex. As the water content increases from low levels to about 5% w/w, dimer formation either remains essentially constant ("QA crystals") or decreases (with "pH 7" crystals). Part of the explanation for this behavior lies in the mechanism for reactivity at

<sup>8</sup> Degradation at 5°C was also studied and is in general agreement with the data at higher temperatures within the precision of the 5°C data. Degradation at 5°C was too small to allow quantitative rate constants to be evaluated.

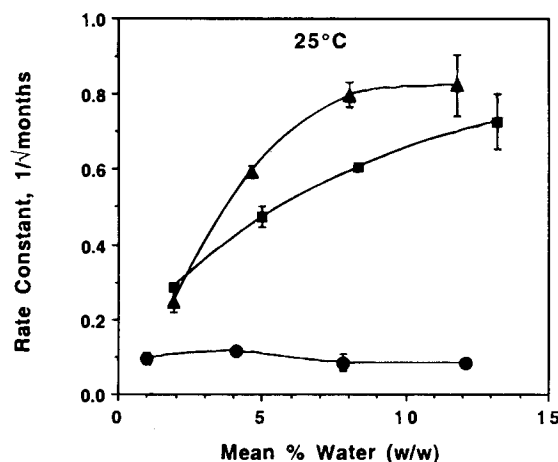
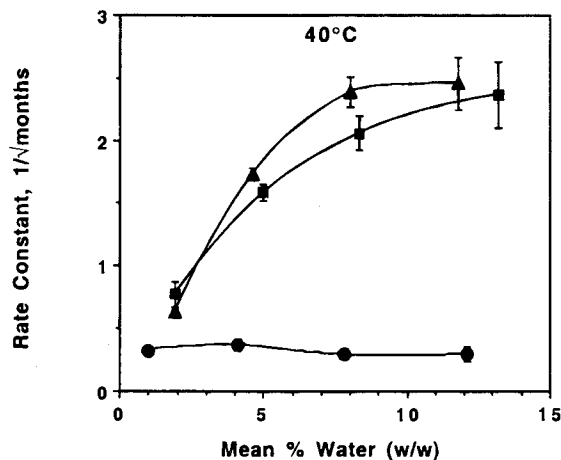


**Fig. 6.** The Effect of Water Content on Rate Constant for A-21 Deamidation of Insulin in the Solid State. The rate constants refer to the pseudo rate constants for "square root of time" kinetics. The standard error in the "rate constants" as determined from the regression analysis are shown as error bars when the error exceeds the size of the plotting symbol.

the A-21 site. The first step in both degradation pathways (i.e., formation of A-21 desamido and dimer) is formation of a cyclic anhydride intermediate with release of ammonia (11). The cyclic anhydride may then either react with water to form the A-21 desamido product or react with an amine from another insulin molecule to form dimers. At least in the pH range of 3–5 with amorphous insulin, formation of the cyclic anhydride is rate determining (11). Thus, at constant rate of anhydride formation, an increase in A-21 desamido formation will mean a corresponding decrease in dimer formation. However, the rate of anhydride intermediate formation does appear to depend on water content. Total degradation in "QA" crystals increases monotonically as the water content increases, and total degradation in "pH 7 crystals" is essentially constant between 2% and 5% water, but increases roughly linearly between 5% and 14% water (data not shown).

#### Comparison with Literature Studies

Previous studies on degradation in solid state insulin have focused either on insulin formulations (5,8,9), which represent

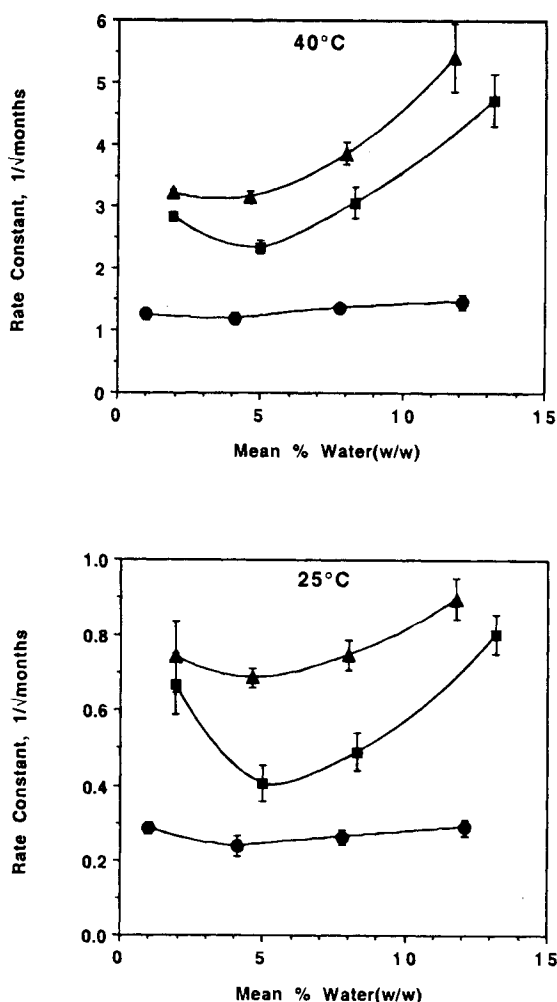


**Fig. 7.** The Effect of Water Content on Rate Constant for Insulin Dimer Formation in the Solid State. Dimer content is measured by the size exclusion HPLC assay. The rate constants refer to the pseudo rate constants for "square root of time" kinetics. The standard error in the "rate constants" as determined from the regression analysis are shown as error bars when the error exceeds the size of the plotting symbol.

aqueous suspensions at neutral pH, or have studied freeze dried insulin preparations at selected water contents in the acid pH range (i.e., pH 3–5 for the solutions being freeze dried) (11). With insulin formulations, the primary deamidation site is B-3, and crystalline formulations are more stable than amorphous preparations. We find crystalline samples to be less stable than the corresponding amorphous samples at all water contents, and except for the amorphous preparations at 75% relative humidity, deamidation at the A-21 site is much greater than deamidation at the B-3 site. Thus, it appears that degradation pathways in a suspension (i.e., 100% relative humidity) are significantly different than in a solid at lower water content (i.e., up to 75% relative humidity). With freeze dried insulin in the pH range 3–5, the primary deamidation site is A-21, and the degradation rate increases with increasing water content. We find that for freeze dried insulin at pH 7.1, the primary deamidation site is generally A-21, but contrary to the acid pH results (11), we find that degradation rate is essentially independent of water content, at least up to 75% relative humid-

ity. This observation suggests that the effect of water content on the stability of amorphous insulin is quite sensitive to pH.

#### *The Effect of Solid Form on Stability: Possible Mechanisms*

From the viewpoint of FTIR, both dried crystalline and dried amorphous insulin are substantially "denatured", and the heats of denaturation (DSC) suggest the crystalline form is slightly "more native". Thus, from an overall structural viewpoint, one would not expect greatly enhanced stability for the amorphous form. While differences in structure in the solid state are likely responsible for the observed stability differences, the relevant structural differences must be more subtle than "native" vs. "denatured".<sup>9</sup>

With small molecules, there are exceptions to the rule that "crystalline is more stable" when the crystal structure positions two reactive groups in close proximity (4). If one assumes that the crystal structure places an A-21 residue from one hexamer very close to the B-1 residue of a molecule from an adjacent hexamer, or at least allows significant motion to allow close approach, dimer formation would be favored. However, since the rate determining step in both formation of A-21 desamido product and the dimer is believed to be a unimolecular cyclization step to form the cyclic anhydride species, proximity of a B-1 residue should determine only the ratio of products formed (i.e., dimer vs. desamido) and should not impact the overall degradation rate. Assuming that degradation proceeds through the cyclic anhydride intermediate, a slower overall degradation rate of the amorphous form must mean that either the cyclization step at residue A-21 is slower in the amorphous form due to local configurational differences, perhaps involving a neighboring catalytic residue, or the back reaction between the cyclic intermediate and ammonia (i.e., see scheme II) is faster in the amorphous state, perhaps due to slower diffusion of ammonia away from the reactive site in the amorphous state. However, we lack direct evidence for either "mechanism".

#### CONCLUSIONS

Freeze dried amorphous insulin is much more stable than is crystalline insulin at corresponding water contents from near zero to about 15% water. Thus, the "rule" stating that the crystalline phase provides greater stability toward degradation clearly does not apply to insulin, and one must question the "rule" for proteins in general. Although the stability differences may well be a result of structural differences in the solids, neither FTIR spectroscopy nor DSC clarify the mechanism involved.

<sup>9</sup> It should be noted that a preservative induced "coil to helix transition" in the B1-B8 region, while far short of a "denatured to native" transition, does indeed stabilize the B-3 residue toward deamidation (5). With this information, it is tempting to attribute the greater stability of the amorphous form to the slightly greater  $\alpha$ -helix content in the amorphous form relative to the crystalline form (i.e., 50% vs. 41%). However, the A-21 site appears to be the reactive residue in most of the systems studied in this research, and A-21 is a terminal residue separated from the A13-A20 helix by a disulfide link between residues A-20 and B-19 (5). It is not obvious how either helix formation in another region of the molecule or a "more structured" A13-A20 helix would restrict mobility and limit reactivity of the A-21 residue.



## ACKNOWLEDGMENTS

We would like to acknowledge Professor John Carpenter of the University of Colorado for the use of his laboratories for performing the FTIR studies and for numerous helpful discussions regarding the interpretation of FTIR data. We also acknowledge the guidance of Professor A. Dong of Colorado State University in performing the FTIR studies. Finally, we would like to thank Dr. John Beals of Eli Lilly & Co. for many useful discussions regarding conformational properties of insulin.

## REFERENCES

1. M. J. Pikal, A. L. Lukes, J. E. Lang, and K. Gaines. *J. Pharm. Sci.* **67**:767 (1978).
2. T. Oguchi, E. Yonemochi, K. Yamamoto, and Y. Nakai. *Chem. Pharm. Bull.* **37**:3088-3091 (1989).
3. M. J. Pikal. "Freeze Drying of Proteins", in *Peptide and Protein Delivery*, 2nd Edition, V. H. L. Lee, Editor, Marcel Dekker, in press.
4. C. N. Sukenik, J. A. P. Bonapase, N. S. Mandel, R. G. Bergman, P. Lau, and G. Wood. *J. Am. Chem. Soc.* **97**:5290-5291 (1975).
5. J. Brange, L. Langkjaer, S. Havelund, and A. Volund. *Pharm. Res.* **9**:715-726 (1992).
6. S. J. Prestrelski, T. Arakawa, and J. F. Carpenter. *Arch. Biochem. Biophys.* **303**:465-473 (1993).
7. S. J. Prestrelski, K. A. Pikal, and T. Arakawa. *Pharm. Res.* **12**:1250-1259 (1995).
8. J. Brange, S. Havelund, and P. Hougaard. *Pharm. Res.* **9**:727-734 (1992).
9. J. Brange, O. Hallund, and E. Sorensen. *Acta Pharm. Nord.* **4**:223-232 (1992).
10. R. T. Darrington and B. D. Anderson. *J. Pharm. Sci.* **84**:275-282 (1995).
11. R. G. Strickley and B. D. Anderson. *Pharm. Res.*, **13**:1142-1153 (1996).
12. A. Dong, S. J. Prestrelski, S. D. Allison, and J. F. Carpenter. *J. Pharm. Sci.* **84**:415-424 (1995).
13. A. Dong, B. Caughey, W. S. Caughey, K. S. Bhat, and J. E. Coe. *Biochem.* **31**:9364-9370 (1992).
14. L. J. Janis, P. M. Kovach, R. M. Riggan, and J. K. Towns. *Methods in Enzymology.* **271**:86-113 (1996).
15. M. J. Hageman. *Drug Dev. Ind. Pharm.* **14**:2047-2070 (1988).
16. M. J. Pikal, K. M. Dellerman, M. L. Roy, and R. M. Riggan. *Pharm. Res.*, **8**:427-436 (1991).
17. M. J. Pikal, K. Dellerman, and M. L. Roy. *Develop Biol. Standard.* **74**:323-340 (1991).
18. A. T. M. Serajuddin, M. Rosoff, and D. Mufson. *J. Pharm. Pharmac.* **38**:219-220 (1985).
19. J. L. Green, J. Fan, and C. A. Angell. *J. Phys. Chem.* **98**:13780-13790 (1994).
20. B. C. Hancock, S. L. Shamblin, and G. Zografi. *Pharm. Res.* **12**:799-806 (1995).
21. L. N. Bell, M. J. Hageman, and L. M. Muraoka. *J. Pharm. Sci.* **84**:707-712 (1995).
22. I. V. Sochava and O. I. Smirnova. *Food Hydrocolloids.* **6**:513-524 (1993).
23. M. J. Pikal and D. Rigsbee. The relationship between glass transition temperature and stability of freeze dried human growth hormone formulations. AAPS Pharmaceutical Technology Symposium: *Viscoelastic properties of pharmaceutical materials*, AAPS National Meeting, Miami, Florida, Nov. 7, 1995.
24. J. R. Lepock, K. P. Ritchie, M. C. Kolios, A. M. Rodahl, K. A. Heinz, and J. Kruuv. *Biochem.* **31**:12706-12712 (1992).
25. S. J. Prestrelski, N. Tedeschi, T. Arakawa, and J. F. Carpenter. *Biophysical J.* **65**:661-671 (1993).
26. Y. Pocker and S. B. Biswas. *Biochem.* **19**:5043-5049 (1980).
27. H. R. Costantino, K. Griebenow, P. Mishra, R. Langer, and A. M. Klibanov. *Biochim. Biophys. Acta.* **1253**:69-74 (1995).
28. C. A. Angell. *J. Non-Cryst. Solids.* **102**:205-221 (1988).
29. R. G. Strickley. Stability of human insulin: Effect of water content and added excipients on the degradation of lyophilized insulin at acidic pH. *Ph.D. Dissertation, The University of Utah.* December, 1995.